Applied Physics Letters

Sensitivity enhancement of a resonant mass sensor based on internal resonance

Cite as: Appl. Phys. Lett. **113**, 223505 (2018); https://doi.org/10.1063/1.5057439
Submitted: 14 September 2018 . Accepted: 10 November 2018 . Published Online: 28 November 2018

Tianyi Zhang, Xueyong Wei, Zhuangde Jiang, and Tianhong Cui

Sensitivity enhancement of a resonant mass sensor based on internal resonance

Tianyi Zhang,[1,2] Xueyong Wei,[1,a)] Zhuangde Jiang,[1] and Tianhong Cui[2,b)]
[1]*State Key Laboratory for Manufacturing Systems Engineering, Xi'an Jiaotong University, Xi'an 710049, China*
[2]*Department of Mechanical Engineering, University of Minnesota, Minneapolis, Minnesota 55455, USA*

(Received 14 September 2018; accepted 10 November 2018; published online 28 November 2018)

There exist numerous vibration modes in a resonant structure, and these modes can interact with each other. Here, the internal resonance between the fundamental mode and higher order modes is observed in a polyvinylidene fluoride piezoelectric membrane as a resonant mass sensor. Higher order modes draw energy from the fundamental one and vibrate at integer times of the fundamental mode's frequency. The resonance frequency shift of the fundamental mode can thus be magnified integer times through internal resonance. The sensitivity of the resonant mass sensor, defined by the resonance frequency shift caused by mass change, is enhanced based on this mechanism. The sensing characteristics are experimentally studied with a concentrated mass load attached to the sensor. The sensitivity improvement of directly using higher order modes and detecting the internal resonance response is tested and compared in our experiment. An 11 times sensitivity magnification is achieved with the internal resonance method, which has an obvious advantage over the higher order method. *Published by AIP Publishing*. https://doi.org/10.1063/1.5057439

Resonant mass sensors are devices that track the resonance frequency shift induced by mass adsorption. Such devices have drawn much attention in biosensor applications for their high sensitivity, label-free operation, low cost, rapid detection, and adaption to various environments.[1–3] The sensitivity of such sensors is defined by the shift of the resonance frequency caused by the attached mass. In general, resonant sensors are designed to operate in the first fundamental mode, but a resonant structure can support numerous vibration modes. Enhancement of sensing properties utilizing a multimode system has been reported in several studies.[4–6] Higher order modes have also been experimentally confirmed to have better mass sensitivity than the fundamental mode in cantilever beams[7–9] and membranes.[10–12] In particular, when different modes have identical or integer multiple frequencies, energy will be exchanged between modes resulting in complicated dynamic phenomena, usually called internal resonance.[13] There has been considerable interest in these special dynamic characteristics in recent years, and researchers have experimentally studied the internal resonance system with mode frequency ratios of 1:1,[14–16] 2:1,[17–21] 3:1,[19] and even 23:1[22] between the directly driven mode and the internal resonance mode. The opposite situation where the higher frequency mode draws energy from the lower frequency mode is also reported with a frequency ratio of 1:2[15,23] and 1:3.[24,25] Some extraordinary properties such as frequency stabilization and amplitude saturation[18,25] are found in the internal resonance system, which has a potential prospect to improve the performance of resonators and oscillators. However, there is no research focusing on magnifying the sensitivity of resonant mass sensors by detecting the internal resonance response.

In this letter, a piezoelectric membrane made of polyvinylidene fluoride (PVDF) is fabricated into a resonant mass sensor. Since the piezoelectric property of PVDF was first reported in 1969,[26] this new piezoelectric material has drawn continual attention due to its mechanical flexibility, lower cost, and faster fabrication.[27,28] Among them, the PVDF membrane resonator is studied for sensors and actuators.[29–32] Here, various vibration modes of the PVDF piezoelectric membrane resonator are identified and their concentrated mass sensitivity is experimentally studied with two methods. Figures 1(a) and 1(b) show a cross-sectional schematic view and a photo of the resonant mass sensor used in our experiment. The fabrication process consists of three steps: (1) two poly (methyl methacrylate) (PMMA) supports are holed to release the vibrating part and electrode with a laser cutter. The dimension of the hollow rectangle is 15 mm long and 10 mm wide. (2) A PVDF film (Measurement Specialties Inc.), with 28 μm and 6 μm thickness of the PVDF material and silver ink printed electrode on both sides, is firmly attached between two PMMA supports with epoxy. (3) Two wires are bonded to silver electrodes to conduct the actuation signal. The experimental setup is schematically shown in Fig. 1(c), where two electrodes are connected to a piezoelectric amplifier; thus, a computer controlled alternating signal is amplified to drive the piezoelectric membrane into vibration. The vibrating motion is measured by a He-Ne laser vibrometer (PSV-400 Polytec Inc.). The measurement is conducted at atmospheric pressure and room temperature.

To begin with, various vibration modes are searched based on the average frequency response measured at 57 scanning points uniformly distributed on the membrane, and the result is shown in Fig. 2(a). Thirteen resonance peaks marked in red arrows are observed during the frequency sweep corresponding to thirteen different vibration modes. The mode shapes of these modes are obtained by scanning the membrane while the device is driven at the frequency of each resonance peaks, and shown in the inset of Fig. 2(a). The color scale in mode shape figures represents amplitude,

a)Electronic mail: seanwei@mail.xjtu.edu.cn
b)Electronic mail: cuixx006@umn.edu

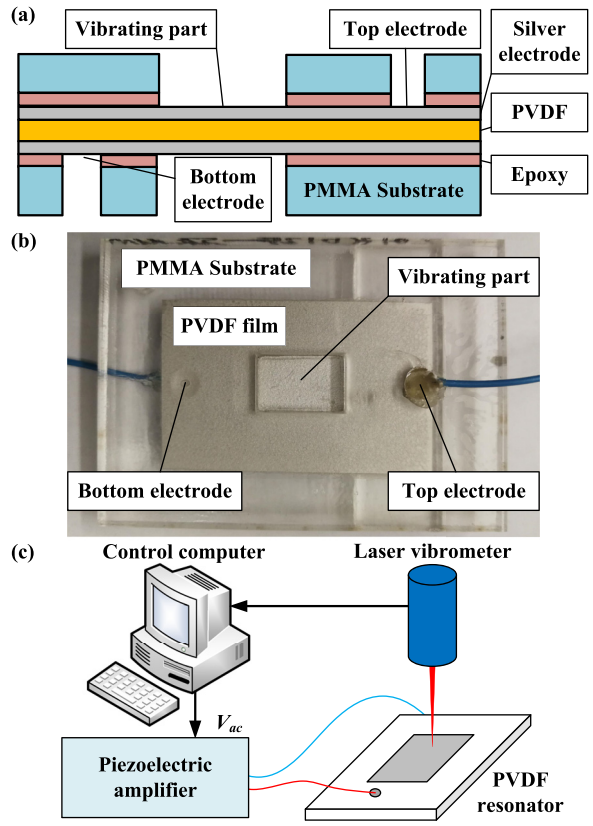

FIG. 1. Cross-sectional schematic (a) and photo (b) of the PVDF piezoelectric membrane resonant mass sensor. (c) The optical measurement setup schematic of the experiment.

and the green parts are node points where the amplitude has the minimum value. Therefore, each vibration mode can be named base on the amount of anti-nodes (shown in red or blue) which have maximum movement distributed along the length and width directions. Then the resonant sensor is driven at the resonance frequency of the fundamental mode $f_{(1,1)}$. A 37×25, in total 925 scanning points grid covering the whole membrane is defined and the frequency spectrum of all these points are measured. The average result is figured out and plotted in Fig. 2(b). Besides the fundamental response at f_r attributed to the direct driving signal, it should be noticed that there exists remarkable response at some integer multiples of driving frequency such as $2f_r$, $3f_r$, $5f_r$, $7f_r$, $9f_r$, and $11f_r$. Mode shapes at the frequency of such a response are calculated and shown in the inset of Fig. 2(b). Noting that the mode shapes measured at integer multiples of the driving frequency are very similar to the ones measured when higher order modes are directly driven [$2f_r$ and (1, 2), $3f_r$ and (2, 2), $5f_r$ and (3, 3), $7f_r$ and (2, 4), $9f_r$ and (1, 5), and $11f_r$ and (6, 4) as are marked in the dashed outline in the same color], which indicates that some specific higher order modes draw energy from the fundamental mode through internal resonance and start to vibrate at the frequency of integer multiples of the driving frequency even though they are not directly driven. The specific integer multiples of the driving frequency are close to the resonance frequencies of corresponding higher order modes, which can be observed by comparing Figs. 2(a) and 2(b).

The integer frequency ratio is achieved in the case of internal resonance. It is expected that a frequency shift in the

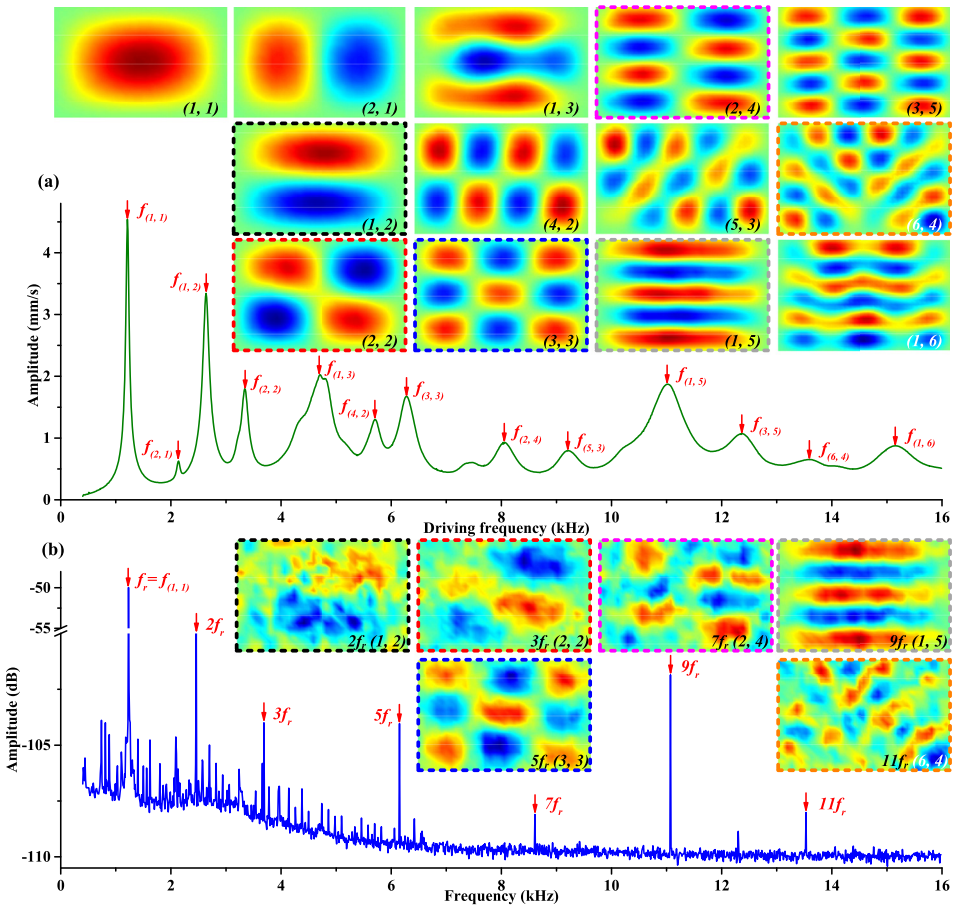

FIG. 2. (a) Frequency response of the membrane resonator where some specific vibration modes are marked with red arrows. The pictures in the inset show the measured mode shapes when the device is directly driven at the resonance frequencies of each marked vibration modes. (b) Frequency spectrum of the resonator while the driving frequency f_r is fixed at the resonance frequency of the fundamental mode $f_{(1,1)}$. The internal resonance response at several multiple frequencies is identified by red arrows. The inset shows the mode shapes measured at the frequency of each internal resonance response. $V_{ac} = 0.3$ V in both measurements.

fundamental mode will lead to integer times frequency shift response at higher order modes during the internal resonance, thus the sensitivity of the sensor can be improved. Besides this method, directly driving higher order modes to detect mass change is first tested to make a comparison. The concentrated mass load is achieved by attaching carbon layers with a dimension of 1×1 mm on the surface of the membrane, as shown in Fig. 3(a). We first measure the mass of a large carbon layer with a width and length of 11.88 and 76.00 mm, respectively, and its weight is 103.7 mg obtained by an analytical balance. Thus, the mass of a single 1×1 mm carbon layer is calculated as approximately 0.115 mg. In order to maximize the resonance frequency shift of the fundamental mode, the masses are attached layer by layer at the only anti-node point of the fundamental mode measured in Fig. 2(a). The frequency response is measured after every two layers are attached to figure out the frequency shift of different vibration modes. The result of the fundamental mode is shown in Fig. 3(b). As can be seen, the resonance peak is obviously moving towards lower frequency as the mass increases. The resonance frequency of the fundamental mode with different attached masses is calculated by tracking the peak frequency of Lorentz fitting curves of the measured frequency response. The resonance frequency shifts of some higher order modes as a function of mass load are obtained in the same way and the results are plotted in Fig. 3(c). The mass sensitivity S_D of each mode is obtained by the linear fit and the results are shown in Table I. In membrane resonant mass sensors, higher resonance frequency generally corresponds to higher mass sensitivity in the uniform mass distributed condition and the sensitivity improvement magnification approximately equals to the frequency ratio of the higher order mode to the fundamental mode.[10–12] However, in the case of concentrated mass load, the mass could be located near node points or anti-node points. The sensing ability of specific higher order modes [(2, 1) and (1, 2)] is worse than the fundamental mode and even insensitive to mass change [(2, 2)]. There are still higher order modes that have better sensitivity than the fundamental mode [(1, 3), (3, 3), and (3, 5)], but the sensitivity improvement magnification is less than the frequency ratio as is shown in Table I. Directly using higher order modes makes no significant sensitivity improvement when the mass is concentrated in a small area.

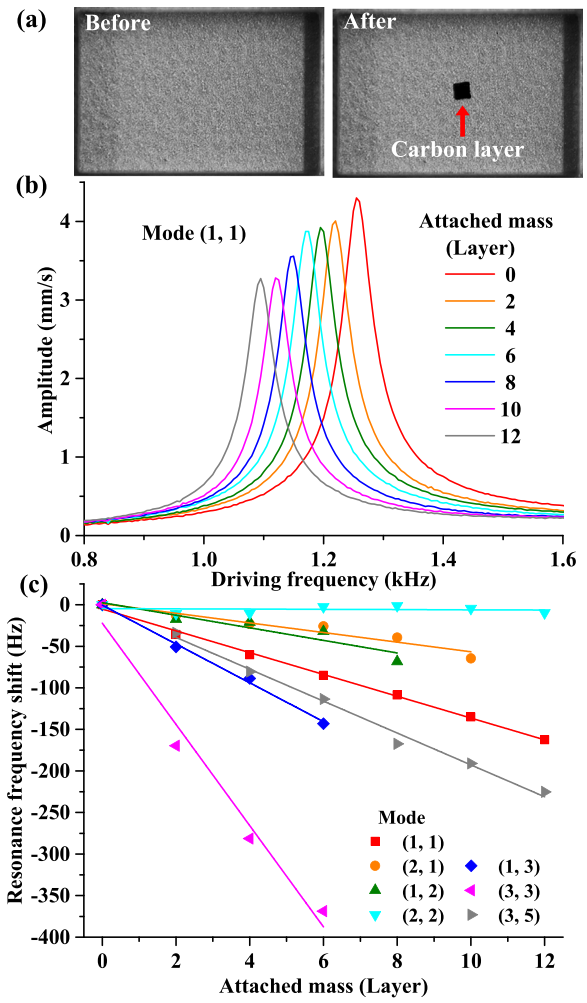

FIG. 3. (a) Photos of the membrane resonator before and after carbon layers are attached. In total, 12 carbon layers are attached layer by layer in this experiment. (b) Measured frequency response curves of the fundamental mode with different attached masses. (c) Resonance frequency shift of the fundamental mode and some specific higher order modes as a function of the number of attached carbon layers. In this experimental, $V_{ac} = 0.3$ V.

To investigate the sensing characteristics of the internal resonance method, the frequency spectrum is measured under each mass load. In each measurement, the device is driven at the resonance frequency of the fundamental mode in Fig. 3(b), and the results are shown in Fig. 4. As is observed in Fig. 4(a), during the response peak of the fundamental mode shifts induced by mass change, an exact 2, 3, and 5 times frequency shift is achieved in the internal resonance response at higher order modes. A similar 7, 9, and 11 times frequency shift can be found in Fig. 4(b). Hence, the vibrating frequency shift of the fundamental mode is magnified integer times by measuring the internal resonance response at certain higher-order modes. In other words, the sensitivity of the resonant mass sensor is improved by integer times with this method. The mass sensitivity of the internal resonance method S_{IR} is also filled in Table I to make comparison. In the previous testing method, higher order modes are directly driven and detected. The higher the order, the more complicated the mode shape, which unavoidably leads to a declination in sensitivity to concentrated mass load. In contrast, if internal resonance is employed, the sensor works at the fundamental mode and internal resonance response at integer times frequency is detected. The sensitivity improvement magnification maintains at the integer close to the frequency ratio of the higher order mode to the fundamental mode regardless of mass distribution. Although 11 times magnification is achieved in this test, it is possible to improve this value by detecting the internal resonance at even higher order modes.

To conclude, the sensing characteristics of the PVDF membrane-based resonant mass sensor are experimentally studied in our work. Piezoelectric actuation and the optical detection method are utilized. Internal resonance between the fundamental and higher order modes is observed when the device is driven at the resonance frequency of the fundamental mode. The higher order modes draw energy from the fundamental mode and vibrate at integer times of the driving frequency. A frequency shift magnification mechanism is

TABLE I. Resonance frequency of different modes and mass sensitivity obtained by the direct and internal resonance methods.

Mode	(1, 1)	(2, 1)	(1, 2)	(2, 2)	(1, 3)	(3, 3)	(2, 4)	(1, 5)	(3, 5)	(6, 4)
Resonance frequency, f_r (Hz)	1255.8	2208.9	2710.3	3427.1	4771.9	6430.5	8177.9	11 136	1 2601	13 938
Frequency ratio, $f_r/f_{r(1,1)}$	1	1.76	2.16	2.73	3.80	5.12	6.51	8.87	10.03	11.10
Mass sensitivity, S_D (Hz/layer)	−13.12	−5.79	−7.56	−0.15	−23.35	−60.89	…	…	−19.18	…
Mass sensitivity, S_D (Hz/mg)	−114.19	−50.41	−65.82	−1.28	−203.28	−530.13	…	…	−166.96	…
Sensitivity ratio, $S_D/S_{(1,1)}$	1	0.44	0.58	0.01	1.78	4.64	…	…	1.46	…
Mass sensitivity, S_{IR} (Hz/Layer)	…	…	−26.23	−39.35	…	−65.58	−91.81	−118.04	…	−144.27
Mass sensitivity, S_{IR} (Hz/mg)	…	…	−228.39	−342.58	…	−570.97	−799.36	−1027.75	…	−1256.14
Sensitivity ratio, $S_{IR}/S_{(1,1)}$	…	…	2	3	…	5	7	9	…	11

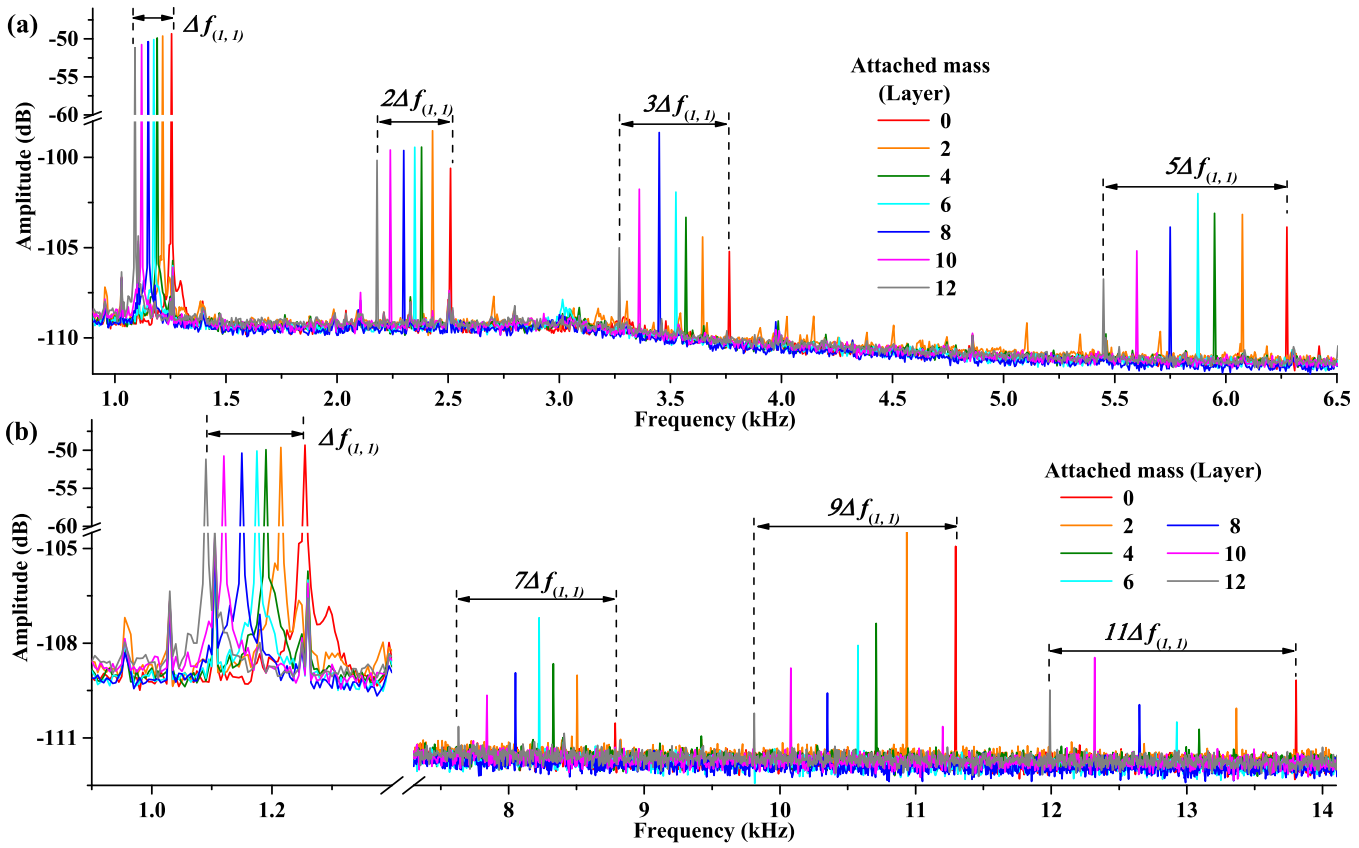

FIG. 4. (a) and (b) Frequency spectrum of the resonant mass sensor under various attached masses. In each measurement, the device is driven at the resonance frequency of the fundamental mode after the mass is attached. $V_{ac} = 0.3$ V in this measurement.

then achieved, and thus the sensitivity of the resonant mass sensor can be magnified integer times through internal resonance. Compared with directly measuring higher order modes, the internal resonance method has an obvious advantage in concentrated mass detection.

This work was financially supported by the National Natural Science Foundation of China (51575439), the 111 Project (B12016), and the China Scholarship Council. We also appreciate the support from Anderson Innovation Labs at the University of Minnesota.

[1]J. Arlett, E. Myers, and M. Roukes, Nat. Nanotechnol. **6**, 203 (2011).
[2]S. Pramanik, B. Pingguan-Murphy, and N. A. Osman, Int. J. Electrochem. Sci. **8**, 8863 (2013).
[3]G. Blanco-Gomez, E. Trioux, and V. Agache, IEEE Electron Device Lett. **33**, 609 (2012).
[4]M. S. Hanay, S. I. Kelber, C. D. O'Connell, P. Mulvaney, J. E. Sader, and M. L. Roukes, Nat. Nanotechnol. **10**, 339 (2015).
[5]M. Spletzer, A. Raman, and R. Reifenberger, Appl. Phys. Lett. **91**, 184103 (2007).
[6]P. Thiruvenkatanathan, J. Yan, J. Woodhouse, A. Aziz, and A. Seshia, Appl. Phys. Lett. **96**, 081913 (2010).
[7]M. K. Ghatkesar, V. Barwich, T. Braun, J.-P. Ramseyer, C. Gerber, M. Hegner, H. P. Lang, U. Drechsler, and M. Despont, Nanotechnology **18**, 445502 (2007).
[8]H. Yu and X. Li, Appl. Phys. Lett. **94**, 011901 (2009).
[9]B. N. Johnson and R. Mutharasan, Biosens. Bioelectron. **32**, 1 (2012).
[10]M. Olfatnia, V. Singh, T. Xu, J. Miao, and L. Ong, J. Micromech. Microeng. **20**, 085013 (2010).
[11]M. Olfatnia, T. Xu, J. Miao, and L. Ong, J. Nanosci. Nanotechnol. **11**, 10460 (2011).
[12]X. Lu, Z. Xu, X. Yan, S. Li, W. Ren, and Z. Cheng, Curr. Appl. Phys. **11**, S285 (2011).
[13]K. Asadi, J. Yu, and H. Cho, Philos. Trans. R. Soc., A **376**, 20170141 (2018).
[14]X. Li, T. Ono, R. Lin, and M. Esashi, Microelectron. Eng. **65**, 1 (2003).
[15]C. Samanta, P. Yasasvi Gangavarapu, and A. Naik, Appl. Phys. Lett. **107**, 173110 (2015).
[16]X. Wei, T. Zhang, Z. Jiang, J. Ren, and R. Huan, Appl. Phys. Lett. **110**, 143506 (2017).

[17]A. Vyas, D. Peroulis, and A. K. Bajaj, J. Microelectromech. Syst. **18**, 744 (2009).
[18]C. Van der Avoort, R. Van der Hout, J. Bontemps, P. Steeneken, K. Le Phan, R. Fey, J. Hulshof, and J. Van Beek, J. Micromech. Microeng. **20**, 105012 (2010).
[19]A. H. Ramini, A. Z. Hajjaj, and M. I. Younis, Sci. Rep. **6**, 34717 (2016).
[20]A. Sarrafan, B. Bahreyni, and F. Golnaraghi, in *19th International Conference on Solid-State Sensors, Actuators and Microsystems (TRANSDUCERS), 2017* (IEEE, 2017), pp. 102–105.
[21]L. Xiong, L. Tang, and B. R. Mace, Nonlinear Dyn. **91**, 1817 (2018).
[22]L. Lipiäinen, A. Jaakkola, K. Kokkonen, and M. Kaivola, Appl. Phys. Lett. **100**, 153508 (2012).
[23]R. Potekin, S. Dharmasena, H. Keum, X. Jiang, J. Lee, S. Kim, L. A. Bergman, A. F. Vakakis, and H. Cho, Sens. Actuators A: Phys. **273**, 206 (2018).
[24]C. Chen, D. H. Zanette, D. A. Czaplewski, S. Shaw, and D. López, Nat. Commun. **8**, 15523 (2017).
[25]D. Antonio, D. H. Zanette, and D. López, Nat. Commun. **3**, 806 (2012).
[26]H. Kawai, Jpn. J. Appl. Phys. Part 1 **8**, 975 (1969).
[27]K. S. Ramadan, D. Sameoto, and S. Evoy, Smart Mater. Struct. **23**, 033001 (2014).
[28]A. Jain, A. K. Sharma, and A. Jain, Polym. Eng. Sci. **55**, 1589 (2015).
[29]D. Zhang and T. Cui, Microsyst. Technol. **19**, 1041 (2013).
[30]N. Tamjidi, K. Sato, J. Sakurai, and S. Hata, IEEJ Trans. Electr. Electron. Eng. **8**, 199 (2013).
[31]B. Zhao, J. Hu, W. Ren, F. Xu, X. Wu, P. Shi, and Z.-G. Ye, Ceram. Int. **41**, S602 (2015).
[32]X. Lu, L. Hou, L. Zhang, Y. Tong, G. Zhao, and Z.-Y. Cheng, Sens. Actuators A: Phys. **261**, 196 (2017).